iScience

CellPress
OPEN ACCESS

Article

Gut Bacterial Species Distinctively Impact Host Purine Metabolites during Aging in *Drosophila*

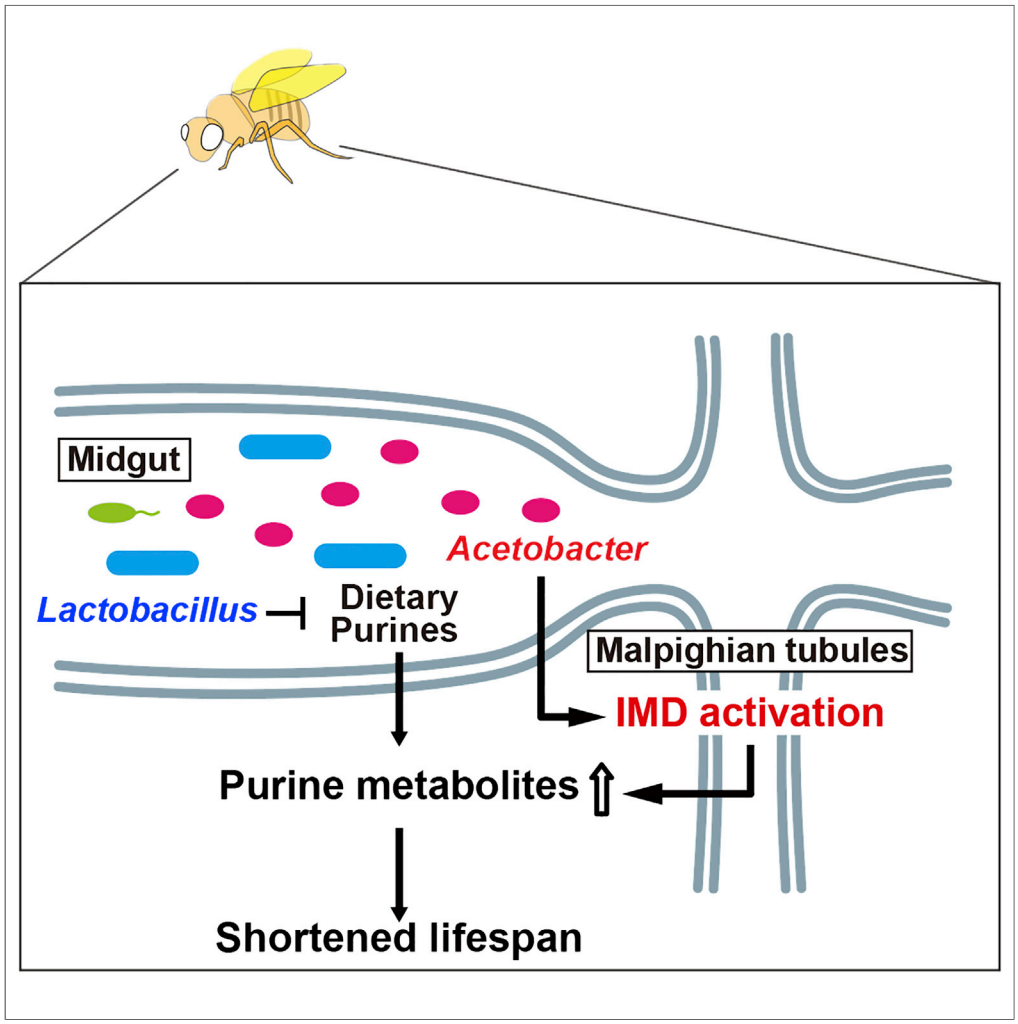

Toshitaka Yamauchi, Ayano Oi, Hina Kosakamoto, ..., Hiroshi Mori, Masayuki Miura, Fumiaki Obata

fumiaki.obata@g.ecc.u-tokyo.ac.jp

HIGHLIGHTS

Gut bacterial species regulate the age-dependent metabolic shift in *Drosophila*

Acetobacter persici increases purine levels via IMD activation in the renal tubules

Lactobacillus plantarum decreases the purine levels in the *Drosophila* diet

Diet- and bacteria-dependent elevation of purine levels may shorten the lifespan

Yamauchi et al., iScience *23*, 101477
September 25, 2020
https://doi.org/10.1016/j.isci.2020.101477

iScience

CellPress
OPEN ACCESS

Article

Gut Bacterial Species Distinctively Impact Host Purine Metabolites during Aging in *Drosophila*

Toshitaka Yamauchi,[1] Ayano Oi,[1] Hina Kosakamoto,[1] Yoriko Akuzawa-Tokita,[1] Takumi Murakami,[2] Hiroshi Mori,[2] Masayuki Miura,[1] and Fumiaki Obata[1,3,*]

SUMMARY

Gut microbiota impacts the host metabolome and affects its health span. How bacterial species in the gut influence age-dependent metabolic alteration has not been elucidated. Here we show in *Drosophila melanogaster* that allantoin, an end product of purine metabolism, is increased during aging in a microbiota-dependent manner. Allantoin levels are low in young flies but are commonly elevated upon lifespan-shortening dietary manipulations such as high-purine, high-sugar, or high-yeast feeding. Removing *Acetobacter persici* in the *Drosophila* microbiome attenuated age-dependent allantoin increase. Mono-association with *A. persici*, but not with *Lactobacillus plantarum*, increased allantoin in aged flies. *A. persici* increased allantoin via activation of innate immune signaling IMD pathway in the renal tubules. On the other hand, analysis of bacteria-conditioned diets revealed that *L. plantarum* can decrease allantoin by reducing purines in the diet. These data together demonstrate species-specific regulations of host purine levels by the gut microbiome.

INTRODUCTION

Commensal bacteria have a profound effect on host health. Gut microbiota can influence the host metabolome, as they modulate dietary components and provide some metabolites directly to the host (Tang et al., 2019; Visconti et al., 2019). It is also possible that some bacterial cues stimulate specific metabolic pathways in the host. However, the detailed connection between the microbiome and the host metabolome, particularly in the context of aging, is only beginning to be identified.

Drosophila melanogaster is a powerful model for the mechanistic elucidation of host-microbiome interaction during aging. The advantages of *Drosophila*, with its abundant genetic tools, include the relatively short lifespan and a small number of indigenous bacterial genera, predominantly *Lactobacillus* and *Acetobacter* (Erkosar et al., 2013; Miguel-Aliaga et al., 2018). The simple bacterial communities, nevertheless, can influence host aging, during which the gut microbiome becomes dysbiotic (Clark et al., 2015; Guo et al., 2014). Several metabolites produced by the *Drosophila* microbiota are known to limit the host lifespan. For instance, some bacterial species, such as *Lactobacillus brevis* or *Gluconobacter morbifer*, produce uracil and elicit intestinal damage (Lee et al., 2013). An expansion of *Lactobacillus plantarum* in the gut of null mutant of the immune regulator *PGRP-SD* shortens the lifespan through lactate (Iatsenko et al., 2018). Although many bacteria-derived metabolites that affect health span have been identified, bacteria-dependent reduction of nutrient in the host diet remains unexplored. Besides, there are still many questions on how microbiota regulate the host metabolic pathways during aging.

Here, we performed metabolome analyses to identify how gut microbiota influence the age-related metabolic trajectory in *Drosophila*. Allantoin was found to be increased during aging in flies with normal microbiome but not with depleted *Acetobacter persici*. We also found that *L. plantarum* reduced purine levels from the fly diet. In this study, we revealed how dietary and bacterial factors regulate allantoin as a marker of total purine levels in the body.

[1]Department of Genetics, Graduate School of Pharmaceutical Sciences, the University of Tokyo, Bunkyo-ku, Tokyo 113-0033, Japan

[2]Department of Informatics, National Institute of Genetics, Mishima, Shizuoka 411-8540, Japan

[3]Lead Contact

*Correspondence: fumiaki.obata@g.ecc.u-tokyo.ac.jp

https://doi.org/10.1016/j.isci.2020.101477

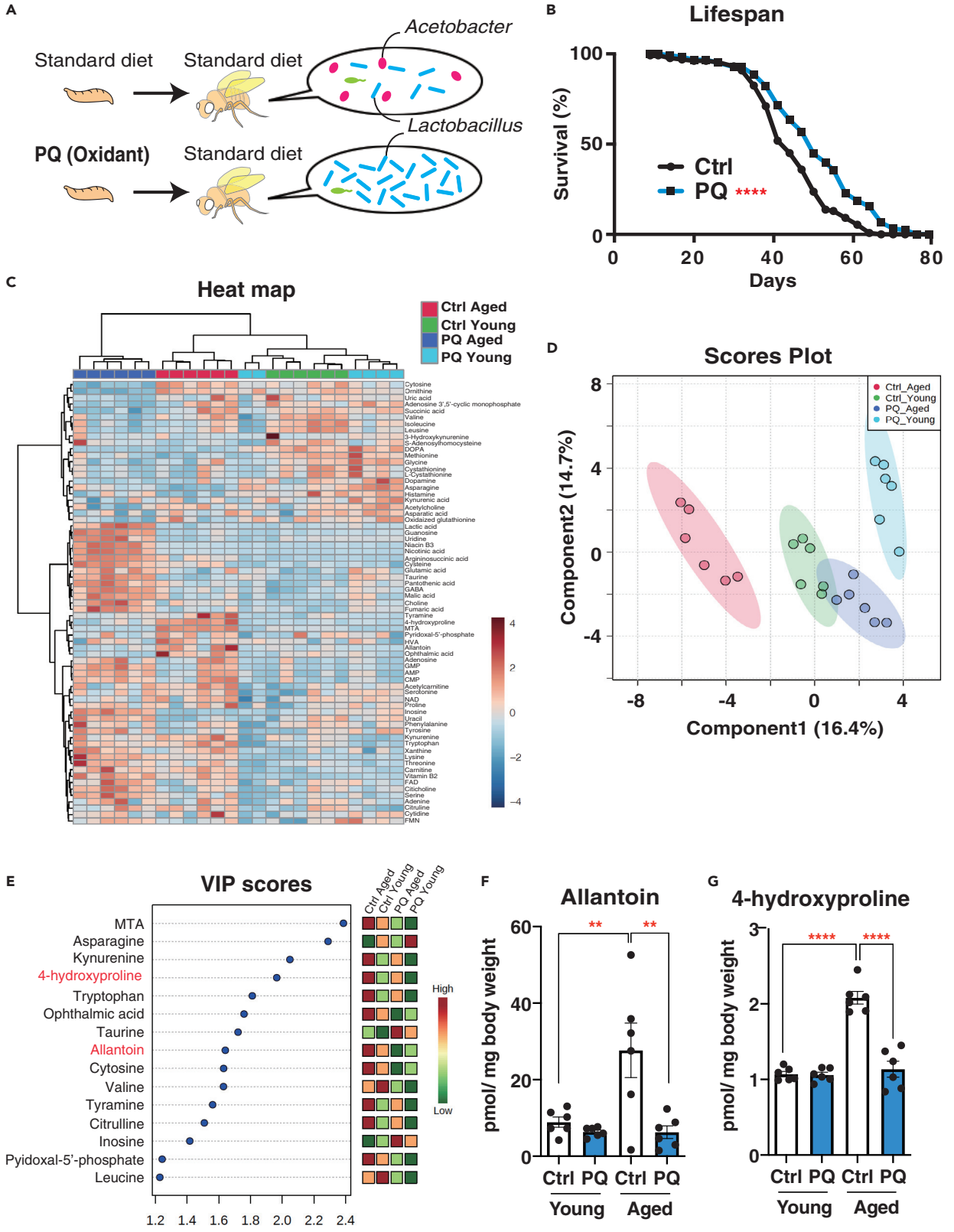
A
Standard diet
Standard diet
Acetobacter
Lactobacillus
PQ (Oxidant)
Standard diet
B
Lifespan
Survival (%)
100
50
0
Ctrl
PQ ****
0
20
40
60
80
Days
C
Heat map
Ctrl Aged
Ctrl Young
PQ Aged
PQ Young
4
2
0
−2
−4
D
Scores Plot
Ctrl_Aged
Ctrl_Young
PQ_Aged
PQ_Young
Component2 (14.7%)
8
4
0
-4
-8
-4
0
4
Component1 (16.4%)
E
VIP scores
Ctrl Aged
Ctrl Young
PQ Aged
PQ Young
MTA
Asparagine
Kynurenine
4-hydroxyproline
Tryptophan
Ophthalmic acid
Taurine
Allantoin
Cytosine
Valine
Tyramine
Citrulline
Inosine
Pyidoxal-5'-phosphate
Leucine
1.2
1.4
1.6
1.8
2.0
2.2
2.4
High
Low
F
Allantoin
pmol/ mg body weight
60
40
20
0
**
**
Ctrl PQ Ctrl PQ
Young
Aged
G
4-hydroxyproline
pmol/ mg body weight
3
2
1
0
****
****
Ctrl PQ Ctrl PQ
Young
Aged

Figure 1. The Altered Microbiome by Oxidant Alters Age-Related Metabolic Trajectory

(A) Overview of phenotypes of the paraquat (oxidant)-experienced flies.

(B) Lifespan of control (Ctrl) or paraquat (PQ)-exposed w^{Dah} male flies. n = 131 (Ctrl), n = 123 (PQ). Log rank test, $p < 0.0001$.

(C–E) Whole body metabolome in young (1-week old) or aged (5-week old) w^{Dah} male flies with or without PQ treatment during larval stage. n = 6. Heatmap (C), PLS-DA analysis (D), and Variable Importance in Projection scores (E) are shown.

(F and G) Quantification of allantoin (F) and 4-hydoxyproline (G) by LC-MS/MS in whole body of young or aged w^{Dah} male flies with or without PQ treatment during larval stage.

Data are represented as mean and SEM. n = 6. Statistics: one-way ANOVA with Sidak's multiple comparison test. **$p < 0.01$. ****$p < 0.0001$.

RESULTS

Microbiome Affects Age-Dependent Metabolic Shift

A previous study showed that low-dose oxidants such as paraquat during development selectively deplete *Acetobacteraceae* and expand *Lactobacillaceae* (Obata et al., 2018). This altered microbiome suppresses age-related immune activation and intestinal dysfunction, leading to lifespan extension (Figures 1A and 1B). To identify how the microbiome remodeling affects the host metabolome during aging, we quantified whole-body metabolites in young or aged male flies with or without oxidant (paraquat) experience. Liquid chromatography/tandem mass spectrometry (LC-MS/MS) was used to quantify metabolites in the whole-body samples from 1-week-old versus 5-week-old flies; at that time the two lifespan curves did not differ significantly (Figure 1B). The analysis enabled us to quantify the 69 metabolites in this setting. A heatmap analysis revealed that the metabolome of paraquat-experienced young flies was not separated well from that of control flies (Figure 1C, green versus light blue). When the flies were aged, in contrast, the cluster between the two conditions became distinct (Figure 1C, red versus blue). Furthermore, a partial least squares discriminant analysis (PLS-DA) showed that the metabolome of control flies strongly shifted during aging along with the component 1 axis, whereas that of paraquat-experienced flies did not (Figure 1D). These data implied that the gut microbiome influenced the flies' "age-dependent" metabolic trajectory.

Among the top 15 metabolites in Variable Importance in Projection scores, which are used in a PLS model to estimate a possible variable for the division among conditions (Figure 1E), we found that allantoin and 4-hydroxyproline were robustly increased during aging in all tested "control" strains, $w^{Dahomey}$, *Canton S*, and w^{iso31} (Figures 1F, 1G, S1A, and S1B). The increases of these two metabolites during aging were suppressed by early-life paraquat exposure (Figures 1F and 1G). Thus, these metabolites were regulated in a bacteria-dependent manner. Neither allantoin nor 4-hydroxyproline feeding shortened the lifespan, suggesting that these metabolites *per se* were not detrimental for flies (Figures S1C and S1D). Therefore, we decided to understand the mechanism regarding how these metabolites were increased during aging.

Allantoin Is Synthesized upon Increase of the Total Purine Levels

Allantoin is an end product of purine degradation pathway in *Drosophila* (Figure 2A). In humans, excess purine bodies are metabolized into uric acid to excrete them from the body. Many other animals, including mice and flies, have functional urate oxidase (Uro), which enables further degradation of uric acid into allantoin. We first hypothesized that the age-dependent accumulation of allantoin might be due to the dysfunction of the excretion process. We conducted an "excretion assay" using blue-dye food (Figure S2A, Shell et al., 2018). Unexpectedly, the total capacity of excretion did not decrease during aging (Figure S2B). We quantified allantoin levels in collected excreta using LC-MS/MS to test whether allantoin excretion was specifically defective in the aged flies. The amount of allantoin in excreta was not decreased, rather it was slightly increased (Figure S2C), suggesting that old flies were capable of, more or less, excreting the metabolite. Theoretically, an increase of food intake can upregulate allantoin levels. However, the capillary feeder assay (Ja et al., 2007) showed that food intake was decreased during aging rather than increased (Figure S2D).

Next, we tested whether allantoin synthesis was upregulated in the aged flies. *Drosophila Uro* is predominantly expressed in the Malpighian tubules, the fly counterpart of renal tubules (flybase.org). Gene expression of allantoin synthase *Uro* as well as its up- and downstream enzymes, *Rosy* and *CG30016*, was not increased, at least transcriptionally, during aging in the Malpighian tubules (Figures 2A and S2E). Thus, the upregulation of total purine levels, or its flux, is likely to be a cause of the age-related increase of allantoin. Interestingly, when we quantified each purine metabolite in young male flies, we noticed that the basal level of allantoin was relatively low compared with that of uric acid (Figure 2B). It is believed that a majority of excess purines, or nitrogen generally, are excreted in the form of allantoin. However, this pattern was also the case in the excreta metabolites, suggesting that uric acid, not allantoin, is excreted despite flies having functional Uro (Figure 2C).

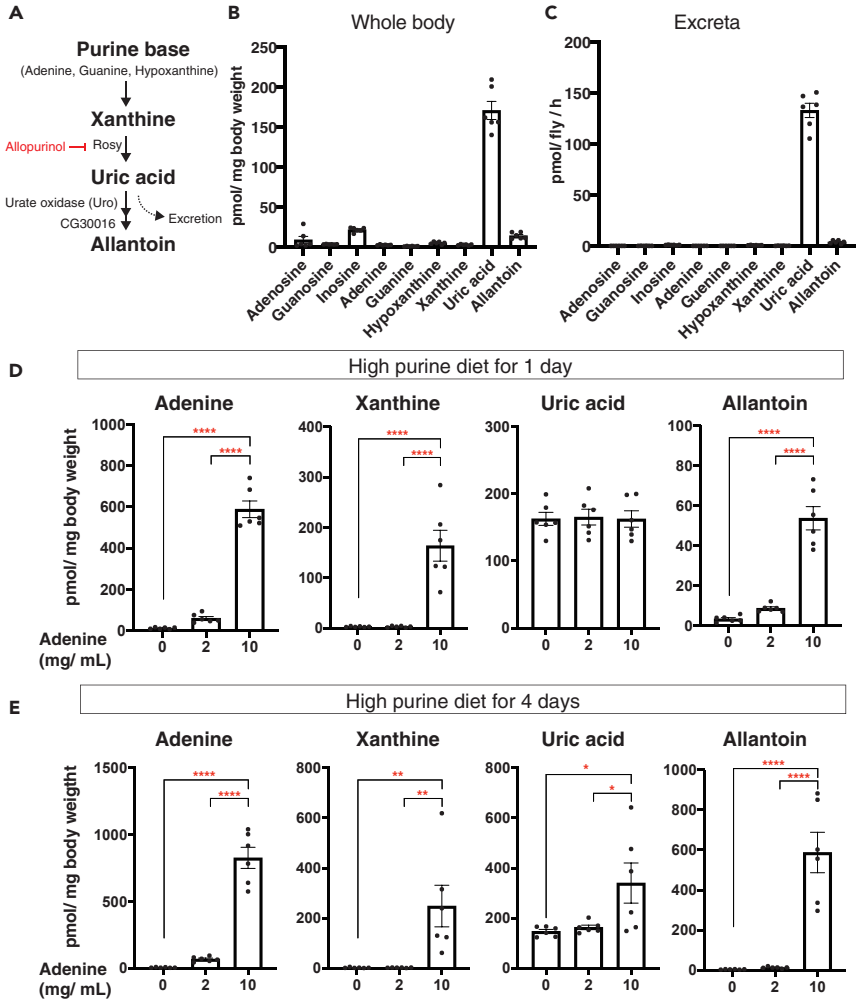

Figure 2. Allantoin Is Produced upon Excessive Purines

(A) Purine metabolism in *Drosophila melanogaster*.

(B and C) Quantification of purine metabolites by LC-MS/MS in whole body (B) or excreta (C) of young (1-week-old) w^{Dah} male flies. n = 6.

(D and E) Quantification of adenine, xanthine, uric acid, and allantoin by LC-MS/MS in whole body of young (2-week-old) w^{Dah} male flies fed with a high-purine diet for 1 day (D) or 4 days (E). n = 6.

Data are represented as mean and SEM. Statistics: one-way ANOVA with Tukey's multiple comparison test. *p < 0.05. **p < 0.01. ****p < 0.0001.

To characterize the allantoin metabolism in flies, we fed male flies with allopurinol, an inhibitor of xanthine oxidase used for treating hyperuricemia in humans (Figure 2A). Both uric acid and allantoin in the whole body were decreased, whereas xanthine was increased (Figure S3A). On the other hand, feeding young male flies with a high-adenine diet led to an increased allantoin, uric acid, and xanthine in a dose- and duration-dependent manner (Figures 2D and 2E). The allantoin level in the excreta was also elevated upon adenine feeding, whereas uric acid was rather decreased for an unknown reason (Figure S3B).

The increased allantoin level by adenine feeding was correlated with shortened lifespan (Figure S3C), consistent with the previous report (van Dam et al., 2020). Other dietary nutrients, such as sugars and amino acids, can provide with substrates for purine biosynthesis. A high-sugar diet causes early mortality due to the increased uric acid production and concomitant renal stones in flies (van Dam et al., 2020). High-yeast feeding also induces uric acid accumulation and shortens the lifespan of *Uro* knockdown flies (Lang et al., 2019). As expected, allantoin, as well as xanthine and uric acid, was increased in whole body by both dietary manipulations (Figures 3A and 3B). Taken together, the allantoin level in flies is commonly elevated upon

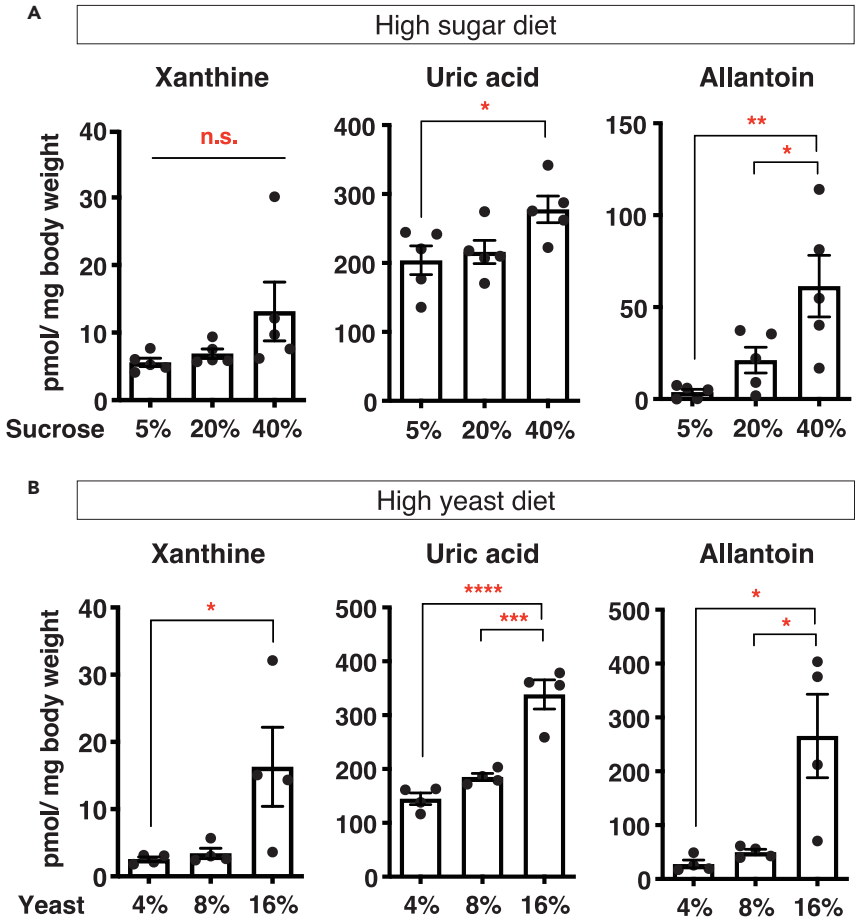

Figure 3. High-Sugar and High-Yeast Diets Increase Allantoin

(A and B) Quantification of xanthine, uric acid, and allantoin by LC-MS/MS in whole body of young (1-week-old) w^{Dah} male flies fed with a high-sugar diet (A, n = 5) or a high-yeast diet (B, n = 4) for 3 days. Data are represented as mean and SEM. Statistics: one-way ANOVA with Tukey's multiple comparison test. *p < 0.05. **p < 0.01. ***p < 0.001. ****p < 0.0001.

these lifespan-shortening dietary conditions. During aging, adenosine and xanthine, as well as allantoin, were increased in male flies at 5 weeks of age, although adenine and uric acid were not (Figure S3D). The increased allantoin in aged flies might be due to the increased total purine levels. It is possible that uric acid levels are maintained during aging because allantoin synthesis can buffer the increased purine metabolite levels to a certain extent. We assume that uric acid can also elevate during aging when the total purine levels are beyond the animals' capacity to handle.

Lactobacillus plantarum Decreases Dietary Purines

Purines are either synthesized in cells or ingested as nutrients. Considering that the microbiome possesses its unique metabolic pathways, commensal bacterial species can modulate the purine levels in the *Drosophila* diet. To test this possibility, we conducted a bacterial-conditioning assay (Figure 4A). Bacterial isolates were added to standard fly diets and incubated at 25°C for 24 hours. The composition of this conditioned diet was assessed by LC-MS/MS. In this experiment, we used *Lactobacillus plantarum* Lsi and *Acetobacter persici* Ai, both of which were previously isolated in our laboratory (see Methods). Given that removing *Acetobacteraceae* by paraquat reduces allantoin in aged flies (Figure 1F), it was expected that *A. persici* Ai would produce purines. However, *A. persici* Ai did not increase purines in the diet, except for hypoxanthine; but rather, mildly decreased purine nucleosides, adenosine and guanosine (Figures 4B–4H).

Surprisingly, we observed a sharp reduction of all three purine nucleosides by conditioning with *L. plantarum* Lsi (Figures 4B–4D). Not only purine nucleosides but also purine bases (adenine and guanine),

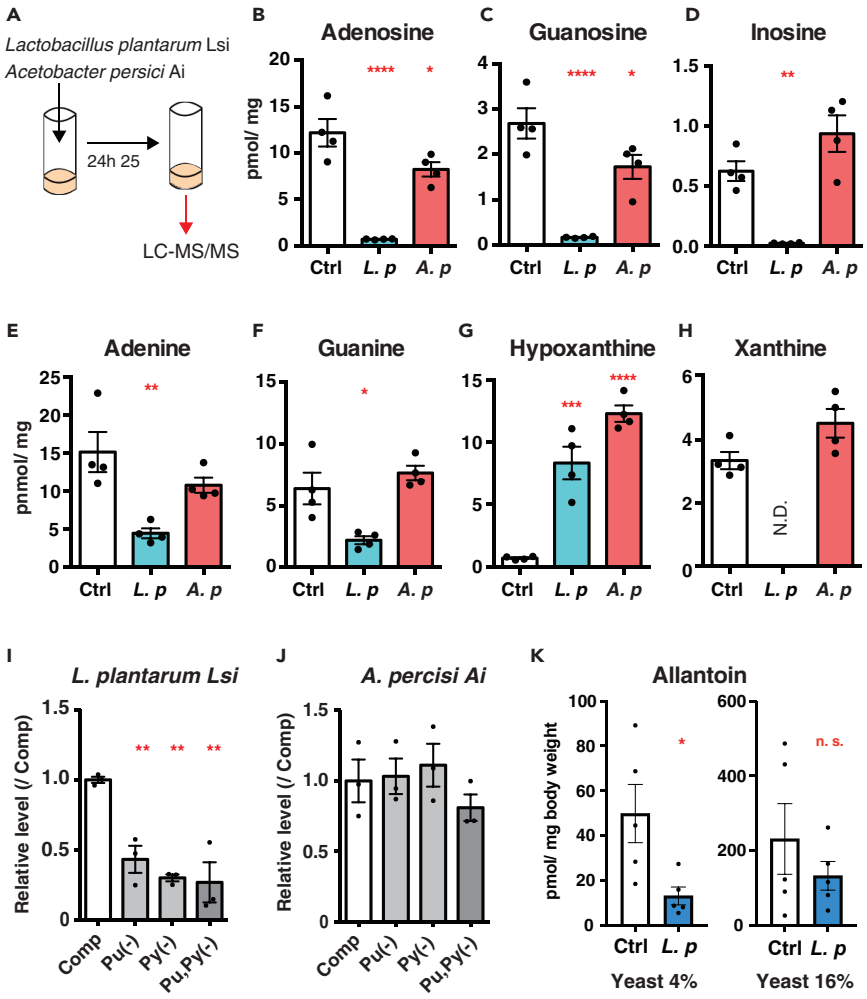

Figure 4. *Lactobacillus Plantarum* Decreases Purine Metabolites

(A) Experimental scheme of bacterial conditioning assay.

(B–H) Quantification of (B) adenosine, (C) guanosine, (D) inosine, (E) adenine, (F) guanine, (G) hypoxanthine, and (H) xanthine by LC-MS/MS in bacterial-conditioned diet with isolated strains. Ctrl, bacterial culture medium; *L. p*, *Lactobacillus plantarum* Lsi; *A. p*, *Acetobacter persici* Ai. n = 4.

(I and J) Bacterial growth of *L. plantarum* Lsi (I) and *A. persici* Ai (J) in purine- or pyrimidine-depleted medium during 21 h of incubation. Relative absorbance (600 nm) to complete medium (Comp) are shown. n = 3.

(K) Quantification of allantoin by LC-MS/MS in whole body of young (1-week-old) w^{Dah} male flies fed with bacterial pre-conditioned diet. n = 5.

Data are represented as mean and SEM. Statistics: one-way ANOVA with Dunnett's multiple comparison test (B–J) or a two-tailed Student t test (K). *p < 0.05, **p < 0.01, ***p < 0.001, ****p < 0.0001.

xanthine, pyrimidine nucleosides (cytidine, thymidine, and uridine), and uracil were reduced in the conditioned diet with *L. plantarum* Lsi, whereas hypoxanthine, cytosine, and thymine were not (Figures 4E–4H and S4A–S4F). Allantoin was not detected in any of the conditioned diets. Next, we examined the specificity of the phenotype by testing other *Acetobacter* species, such as *Acetobacter aceti*, *Acetobacter tropicalis*, and *Acetobacter pasteurianus* in a small scale using a 1.5-mL tube (Figure S4G); none of them decreased adenosine (Figure S4H). In contrast, *Lactobacillus brevis*, but not *Lactobacillus acidophilus* and *Lactobacillus murinus*, decreased dietary adenosine (Figure S4I), which suggested that the ability of adenosine reduction is specific to some *Lactobacillus* species.

To understand what determines the capacity to decrease the purine levels, we performed a comparative analysis of the four *Lactobacilli* genomes. *L. brevis* lacked the majority of the genes involved in *de novo* purine

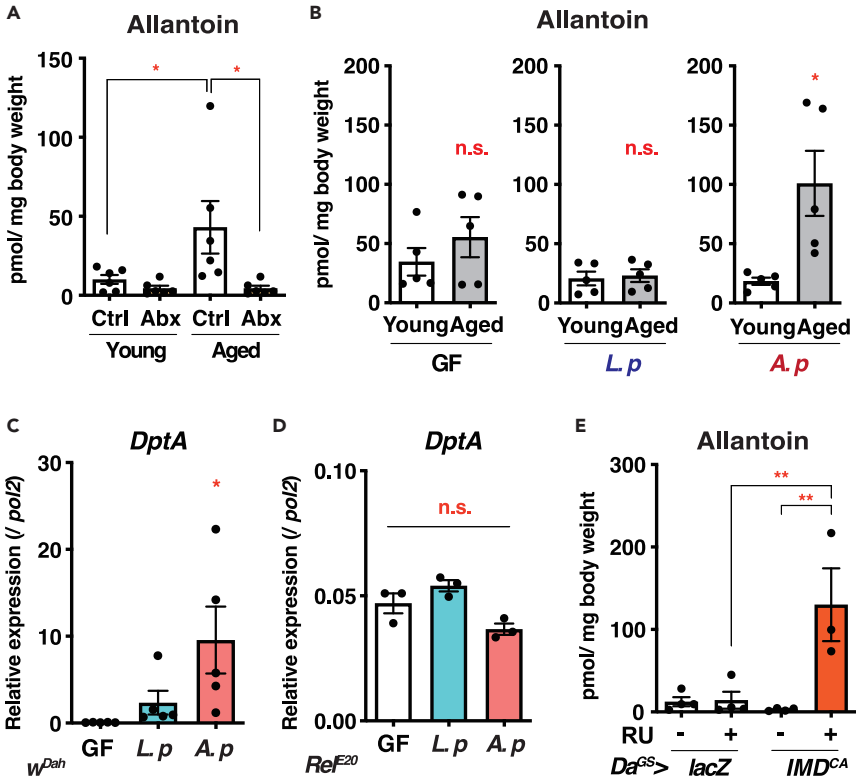

Figure 5. *Acetobacter Persici* Activates IMD and Increases Allantoin during Aging

(A) Quantification of allantoin by LC-MS/MS in whole body of young (2-week-old) or aged (6-week old) w^{Dah} male flies with or without antibiotic treatment. n = 6.

(B) Quantification of allantoin by LC-MS/MS in whole body of young (1-week-old) or aged (5-week-old) w^{Dah} male flies mono-associated with bacterial strains. GF, germ-free; *L.p*, *Lactobacillus plantarum* Lsi; *A.p*, *Acetobacter persici* Ai. n = 5.

(C and D) Quantitative RT-PCR analysis of *Diptericin A* (*DptA*) in whole body of young (1-week-old) male flies mono-associated with the bacterial strains. n = 5 for w^{Dah} flies (C) or n = 3 for *Relish* mutant flies (Rel^{E20}) (D).

(E) Quantification of allantoin by LC-MS/MS in whole body of young (2-week-old) male flies fed with antibiotics. Either *lacZ* or constitutive active form of IMD (IMD^{CA}) was overexpressed ubiquitously by Da^{GS}. RU486 is an inducer of GeneSwitch. n = 3–4.

Data are represented as mean and SEM. Statistics: one-way ANOVA with Sidak's multiple comparison test (A and E), Dunnett's multiple comparison test (C and D), or a two-tailed Student t test (B). *p < 0.05, **p < 0.01.

synthesis, consistent with the fact that this bacterium needed to utilize adenosine in the fly diet. Unexpectedly, not only *L. acidophilus* and *L. murinus* but also *L. plantarum* Lsi possess genes for the *de novo* purine synthesis pathway. We also inspected genes encoding transporters to ask whether specific expression of the transporters explains the difference in purine metabolism. *L. plantarum* Lsi and *L. brevis* had homologs of the purine-cytosine transporter *codB*, whereas the other two strains did not. In contrast, there is a gene for NupC/NupG family nucleoside transporter in the genome of *L. murinus*, *L. brevis*, and *L. plantarum*, whereas *L. acidophilus* possessed a gene set encoding BmpA-NupABC, an ATP-binding cassette transporter for nucleosides. The reason why some but not all *Lactobacillus* species reduced environmental nucleosides was not obvious from the genome comparison.

We noticed that the difference in the ability to decrease purine nucleosides among *Lactobacillus* species was correlated with the speed of bacterial growth (Figure S4J). This observation led to the assumption that *L. plantarum* Lsi could utilize extracellular nucleic acids for rapid growth. To test this hypothesis, we analyzed the bacterial growth on a chemically defined medium (see Methods). The medium contains the nucleosides inosine and uridine as sole purine and pyrimidine sources, respectively. The growth of *L. plantarum* Lsi was suppressed, if not abolished, upon either inosine or uridine depletion (Figure 4I), whereas that of *A. persici* was not affected at all (Figure 4J). These data implied that the gut bacteria *L. plantarum* decreased the purine metabolites of the fly diet by using them for promoting bacterial growth.

To test whether this bacterial metabolism can influence fly metabolome, we fed young flies with *L. plantarum* Lsi-conditioned diet. The bacterial conditioning of the low-yeast diet, but not the high-yeast diet, led to the decrease of allantoin levels in flies (Figure 4K). Therefore, commensal bacterium *L. plantarum* could reduce host purine levels by direct modulation of the host's diet, although this is dependent on dietary condition.

On the other hand, the bacterial-conditioned diet with *A. persici* Ai had a significantly large amount of 4-hydroxyproline (Figure S4K). Given that *Acetobacteraceae* is increased during aging (Guo et al., 2014; Obata et al., 2018), the age-dependent increase of 4-hydroxyproline might be attributable to an elevated amount of direct provision by *A. persici*.

Acetobacter persici Increases Allantoin via IMD Activation

The fact that *L. plantarum* decreases dietary purines suggested that abundant colonization of this bacterium in the paraquat-experienced flies (Figure 1A) might prevent the age-related increase of allantoin. If this is the case, removing this bacterium should result in increased allantoin during aging. Unexpectedly, the elimination of all bacterial species, including *L. plantarum*, by antibiotics suppressed the increase of allantoin (Figure 5A). These data therefore suggested that depletion of *A. persici* suppressed the age-related allantoin elevation. To test whether *A. persici* Ai was sufficient for the phenotype, we performed the gnotobiotic experiment. As we expected, *A. persici* Ai mono-association, but neither germ-free nor *L. plantarum* Lsi mono-association, increased the allantoin level during aging (Figure 5B). These data suggested that *A. persici* Ai was responsible for this phenotype. *L. plantarum* mono-associated flies showed a tendency of low allantoin levels compared with the germ-free flies, implying that the bacterium can contribute to better handling at purine levels during aging.

Drosophila has two innate immune signaling cascades, immune deficiency (IMD) and Toll pathways, the counterparts of mammalian tumor necrosis factor receptor and Toll-like receptor pathways, respectively. The IMD pathway is known to be hyperactivated during aging, which can be attenuated by removing microbiota (Clark et al., 2015; Guo et al., 2014; Obata et al., 2018). In our laboratory condition, aging expands the ratio of *Acetobacteraceae* to *Lactobacillaceae*, at least in w^{iso31} male flies (Figure S5A). Male flies with *A. persici* Ai mono-association showed higher levels of *Diptericin A* (*DptA*) expression, which is one of the readouts for IMD activation (Figure 5C), compared with germ-free or *L. plantarum* Lsi mono-associated flies. This is interesting given that IMD pathway could be activated by DAP-type peptidoglycan found in both gram-negative *A. persici* and gram-positive *Lactobacillus* spp. (Broderick and Lemaitre, 2012). A null mutation for the IMD-regulated transcription factor *Relish* abolished the induction of *DptA* by *A. persici* Ai (Figure 5D). In contrast, *A. persici* Ai did not upregulate a Toll readout *Drosomycin* (*Drs*) (Figure S5B). These data suggested that *A. persici* Ai is a potent activator of the IMD pathway.

To test straightforwardly whether IMD activation was sufficient for the age-dependent increase of allantoin levels, we overexpressed the constitutive active form of IMD (IMD^{CA}) in young male flies under antibiotic treatment. Ubiquitous expression of IMD^{CA} by a drug-inducible GeneSwitch driver (Da^{GS}) triggered a sharp increase of allantoin (Figure 5E).

IMD Activation in the Renal Tubules Increases Allantoin in Aged Flies

IMD pathway is activated predominantly via microbiota-produced peptidoglycan (PGN). Monomeric PGN can activate systemic IMD signaling (Charroux et al., 2018; Myllymäki et al., 2014). Interestingly, IMD activation in the Malpighian tubules, but not in the gut or fat body, increased allantoin (Figures 6A and S5C) and also tended to increase adenine and uric acid (Figure S5D). We confirmed that IMD activation was up-regulated in the aged Malpighian tubules (Figure 6B). Consistent with the phenotypes in aged flies (Figures S2D and S2E), neither gene expressions of allantoin synthesis enzymes nor food intake were increased by IMD activation in the Malpighian tubules (Figures S5E and S5F). The increase of allantoin in Malpighian tubule-specific activation of IMD pathway was correlated with a shortened lifespan (Figure S5G).

When *Relish* was knocked down in the Malpighian tubules, the age-dependent increase of allantoin was suppressed (Figure 6C). We confirmed the phenotype by knocking down *dredd*, a component of IMD pathway (Figure 6C), indicating the requirement of IMD activation in the Malpighian tubules for the increased allantoin during aging. Taken together, the gut microbial species *A. persici* and *L. plantarum*

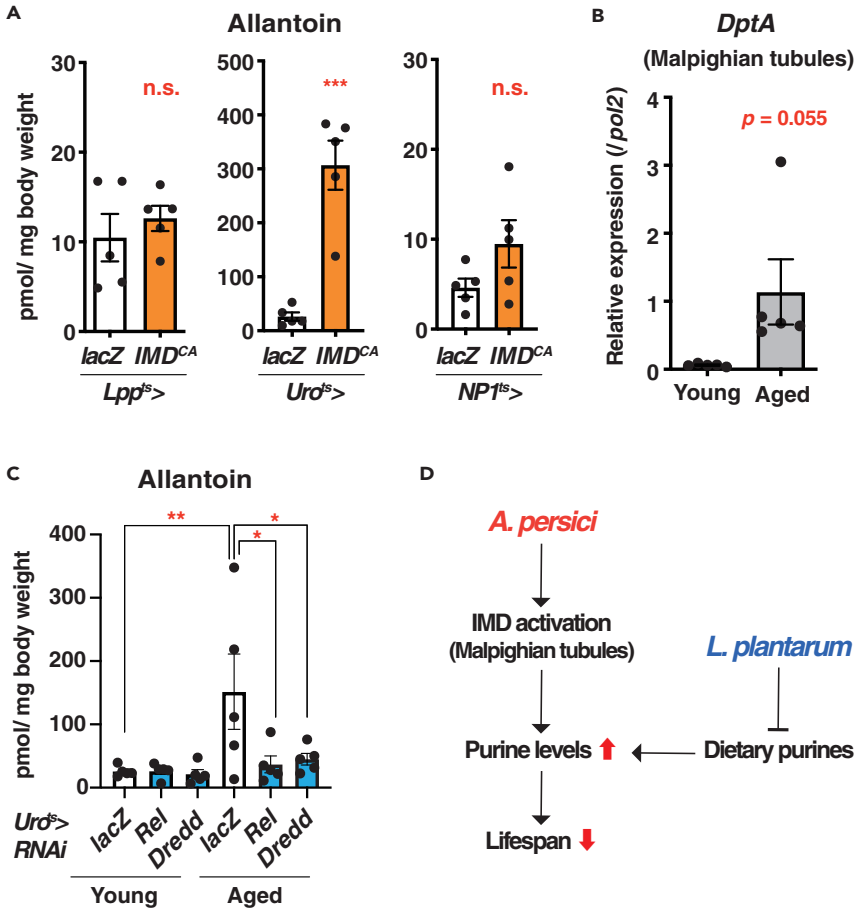

Figure 6. IMD Activation in the Renal Tubules Increases Allantoin

(A) Quantification of allantoin by LC-MS/MS in whole body of young (2-week-old) male flies fed with antibiotics. Constitutive active form of IMD (IMD^{CA}) is overexpressed using tissue-specific drivers (*Lpp-Gal4, tub-Gal80^{ts}*: fat body, *Uro-Gal4, tub-Gal80^{ts}*: Malpighian tubules, *NP1-Gal4, tub-Gal80^{ts}*: gut). n = 5.

(B) Quantitative RT-PCR analysis of *Diptericin A* (*DptA*) in the Malpighian tubules of young (1-week-old) and aged (6-week-old) w^{Dah} male flies. n = 5.

(C) Quantification of allantoin by LC-MS/MS in whole body of young (1-week-old) and aged (4-week-old) male flies with *lacZ*, *Relish*, or *Dredd*-RNAi in the Malpighian tubules. n = 5.

(D) Proposed model.

Data are represented as mean and SEM. Statistics: a two-tailed Student t test (A and B) or one-way ANOVA with Sidak's multiple comparison test (C). *p < 0.05, **p < 0.01, ***p < 0.001.

can influence the age-dependent metabolic trajectory of the purine metabolites, which may contribute to shortening the hosts' lifespan (Figure 6D).

DISCUSSION

Aging impacts metabolic alteration, which is influenced by gut microbiota. Despite the accumulation of descriptive omics data, our mechanistic understanding of age-dependent shift of the metabolome is still in its infancy. This study identified two metabolites, allantoin and 4-hydroxyproline, which were increased during aging in the gut microbiota-dependent manner. The bacterial-conditioning assay demonstrated that 4-hydroxyproline was directly produced by *A. persici* Ai, suggesting that the increase of 4-hydroxyproline is a signature of the expansion of this bacterium during aging. On the other hand, allantoin and many other purine metabolites were not directly produced by any bacterial species. Instead, the immuno-stimulatory capacity of *A. persici* accounts for the age-related increase of allantoin, likely through accelerated purine biosynthesis by the host. Interestingly, a rat model of hyperuricemia-induced nephropathy showed increased levels of uric acid and 4-hydroxyproline, a phenotype similar to our aged *Drosophila* (Pan et al., 2019).

Allantoin is identified as a potential caloric restriction mimetic, and feeding allantoin extends the lifespan in *C. elegans* (Calvert et al., 2016). We noticed that allantoin feeding slightly increased the fly lifespan. However, the elevation of endogenous allantoin by manipulation of dietary sugar, yeast, or purine was correlated with a shortened lifespan. The increase of pro-longevity allantoin can be an adaptive response to aging, or the increase serves simply as a marker for increased total purine levels. Some purines and uric acid levels are also increased in conditions with high allantoin levels, and uric acid accumulation is a cause of shortened lifespan by high-purine diets (van Dam et al., 2020; Lang et al., 2019). It might be interesting to test whether *Uro* overexpression can extend lifespan. Intriguingly, high-sugar diet induces dehydration, and the shortened lifespan of flies with the diet is fully restored by water supplementation (van Dam et al., 2020). High-yeast diet can also induce dehydration, implying that water loss is the common mechanism to increase purine levels by these dietary conditions (Ja et al., 2009). It is also noteworthy that dehydration stress (by decreased environmental humidity) activates innate immunity in the Malpighian tubules (Zheng et al., 2018). Whether the deleterious effect of renal immune activation (Uro^{ts} > IMD^{CA}) on lifespan can be attenuated through water supplementation is worth testing.

Accumulating evidence suggests that chronic activation of inflammatory response is a key driver of aging. In *Drosophila*, systemic or intestinal IMD activation via commensal bacteria is believed to limit the lifespan (Clark et al., 2015; Guo et al., 2014). However, the mechanism by which IMD pathway shortens organismal lifespan is not fully understood. This study implies that the altered purine metabolism is one of the downstream events induced by the systemic IMD pathway. Allantoin is reported to be a biomarker of inflammation in a mouse model of inflammatory bowel diseases (Dryland et al., 2008). In humans, an age-related increase in serum uric acid levels has been widely observed (Dalbeth et al., 2016; Kuo et al., 2015; Kuzuya et al., 2002). Elevated uric acid is associated with many pathologies, including systemic inflammation (Lyngdoh et al., 2011) and mortality (Meisinger et al., 2008). The gut microbiota from patients with gout is significantly different from that of healthy humans (Guo et al., 2016). It is interesting that in goslings, the gut microbiota-derived lipopolysaccharide increased the risk of visceral gout (Xi et al., 2019). Therefore, the gut microbiota-dependent activation of innate immunity might be a general driver of hyperuricemia pathologies and organismal aging in mammals.

The fact that allantoin is increased by IMD activation in the Malpighian tubules implied that tissue- and bacteria-specific mechanisms of immune response impact on the purine metabolism. However, the detail of mechanism by which IMD pathway regulates purine metabolism is not elucidated. Considering that IMD activation does not directly upregulate expression levels of allantoin synthesis enzymes, it might regulate purine synthetic pathways. Purines can be synthesized *de novo* from glucose and amino acids through the pentose phosphate pathway (PPP). It is reported that glycolytic activity was attenuated during aging in *Drosophila* (Ma et al., 2018), potentially increasing glucose flux to PPP. Alternatively, age-dependent acceleration of protein catabolism, possibly via immune activation, can produce free amino acids, leading to an increased purine synthesis to excrete excess nitrogen. This assumption, however, is not supported well by the fact that IMD activation in the gut or fat body, the central metabolic organs, did not increase allantoin levels. In mammals, extracellular adenosine is known to be massively increased during inflammatory conditions via ATP breakdown (Antonioli et al., 2019). How IMD activity in the Malpighian tubules leads to allantoin accumulation is to be investigated in future studies.

Many intrinsic and extrinsic factors, such as age, genotype, or diet, contribute to shaping the bacterial communities (Claesson et al., 2011; Wan et al., 2019). Imbalanced bacterial communities (dysbiosis) compromise health span. Either the direct provision of beneficial bacterium (probiotics) or dietary intervention to increase the beneficial bacterium in the gut (prebiotics) is used to improve human health. Given that microbes release many metabolites, cell wall components, and proteinaceous molecules acting directly on the host tissues, these bacteria-derived factors mediate the beneficial or detrimental effect of the gut microbiome, collectively termed "postbiotics" (Aguilar-Toalá et al., 2018; Suez and Elinav, 2017). In the present study, a bacterial conditioning assay demonstrated the altered nutritional composition, as exemplified by the sharp reduction of purines within 24 hours of bacterial inoculation with *L. plantarum* Lsi. This fermentation of the diet can occur in natural laboratory conditions where the gut microbiome is synchronized to the dietary microbiome. We believe this assay can be used as a model for studying how postbiotics work on the host physiology. Indeed, there are some postbiotic

mechanisms by which *Lactobacillus* spp. suppress uric acid in serum in mice on a high-purine diet (Li et al., 2014). It is interesting to test how much of the postbiotic effect is through reduction, rather than production, of a particular nutrient in the diet.

Limitations of the Study

This study did not directly reveal how increased allantoin levels contribute to organismal aging. We tested allopurinol together with IMD activation in the Malpighian tubules, but failed to rescue the shortened lifespan. This observation was correlated with the accumulation of xanthine, which can also form stones and shorten lifespan. Also, neither the mechanism by which *A. persici* triggers IMD activation in aged animals nor how IMD regulates purine levels was elucidated.

Resource Availability

Lead Contact

Further information and requests for resources and reagents should be directed to and will be fulfilled by the Lead Contact, Fumiaki Obata (fumiaki.obata@g.ecc.u-tokyo.ac.jp).

Materials Availability

All unique/stable reagents generated in this study are available from the Lead Contact without restriction.

Data and Code Availability

The original/source data are available from the Lead Contact on request. The result of 16S rRNA amplicon sequencing analysis has been deposited in DDBJ under the accession number DRA010501.

METHODS

All methods can be found in the accompanying Transparent Methods supplemental file.

SUPPLEMENTAL INFORMATION

Supplemental Information can be found online at https://doi.org/10.1016/j.isci.2020.101477.

ACKNOWLEDGMENTS

We would like to acknowledge Aki Hori, Takayuki Kuraishi, and all the Miura lab members for the technical assistance and critical comments. We thank the NITE Biological Resource Center and Bloomington Drosophila Stock Center for bacteria and fly stocks. This work was supported by AMED-PRIME to F.O. under Grant Number 20gm6010010h0004, by AMED-CREST under Grant Number JP18gm1010006 to H.M., and by AMED-Project for Elucidating and Controlling Mechanisms of Aging and Longevity to M.M under Grant Number JP20gm5010001. This work was also supported by grants from the Japan Society for the Promotion of Science to F.O. under Grant Number 19H03367 and to M.M under Grant Number 16H06385, and by grants from Takeda Science Foundation, Mochida Memorial Foundation for Medical and Pharmaceutical Research to F.O.

AUTHOR CONTRIBUTIONS

F.O. and M.M. conceived the project. T.Y. and A.O. performed experiments and analyzed the data. H.K. established methodology used in the study. Y.A.-T. prepared chemically defined medium for bacteria. T.M. and H.M. analyzed the genome sequences of the bacterial isolates. T.Y. and F.O. wrote the initial manuscript. All authors edited and approved the final manuscript.

DECLARATION OF INTERESTS

The authors declare no competing interests.

Received: February 26, 2020
Revised: July 16, 2020
Accepted: August 17, 2020
Published: September 10, 2020

REFERENCES

Aguilar-Toalá, J.E., Garcia-Varela, R., Garcia, H.S., Mata-Haro, V., González-Córdova, A.F., Vallejo-Cordoba, B., and Hernández-Mendoza, A. (2018). Postbiotics: an evolving term within the functional foods field. Trends Food Sci. Technol. *75*, 105–114.

Antonioli, L., Fornai, M., Blandizzi, C., Pacher, P., and Haskó, G. (2019). Adenosine signaling and the immune system: when a lot could be too much. Immunol. Lett. *205*, 9–15.

Broderick, N.A., and Lemaitre, B. (2012). Gut-associated microbes of Drosophila melanogaster. Gut Microbes *3*, 307–321.

Calvert, S., Tacutu, R., Sharifi, S., Teixeira, R., Ghosh, P., and de Magalhães, J.P. (2016). A network pharmacology approach reveals new candidate caloric restriction mimetics in C. elegans. Aging Cell *15*, 256–266.

Charroux, B., Capo, F., Kurz, C.L., Peslier, S., Chaduli, D., Viallat-lieutaud, A., and Royet, J. (2018). Cytosolic and secreted peptidoglycan-degrading enzymes in Drosophila respectively control local and systemic immune responses to microbiota. Cell Host Microbe *23*, 215–228.e4.

Claesson, M.J., Cusack, S., O'Sullivan, O., Greene-Diniz, R., de Weerd, H., Flannery, E., Marchesi, J.R., Falush, D., Dinan, T., Fitzgerald, G., et al. (2011). Composition, variability, and temporal stability of the intestinal microbiota of the elderly. Proc. Natl. Acad. Sci. U S A *108*, 4586–4591.

Clark, R.I., Salazar, A., Yamada, R., Fitz-Gibbon, S., Morselli, M., Alcaraz, J., Rana, A., Rera, M., Pellegrini, M., Ja, W.W., et al. (2015). Distinct shifts in microbiota composition during Drosophila aging impair intestinal function and drive mortality. Cell Rep. *12*, 1656–1667.

Dalbeth, N., Merriman, T.R., and Stamp, L.K. (2016). Gout. Lancet *388*, 2039–2052.

Dryland, P.A., Love, D.R., Walker, M.F., Dommels, Y., Butts, C., Rowan, D., Roy, N.C., Helsby, N., Browning, B.L., Zhu, S., et al. (2008). Allantoin as A Biomarker of inflammation in an inflammatory bowel disease mouse model: NMR analysis of urine. Open Bioact. Compd. J. *1*, 1–6.

Erkosar, B., Storelli, G., Defaye, A., and Leulier, F. (2013). Host-intestinal microbiota mutualism: "learning on the fly.". Cell Host Microbe *13*, 8–14.

Guo, L., Karpac, J., Tran, S.L., and Jasper, H. (2014). PGRP-SC2 promotes gut immune homeostasis to limit commensal dysbiosis and extend lifespan. Cell *156*, 109–122.

Guo, Z., Zhang, J., Wang, Z., Ang, K.Y., Huang, S., Hou, Q., Su, X., Qiao, J., Zheng, Y., Wang, L., et al. (2016). Intestinal microbiota distinguish gout patients from healthy humans. Sci. Rep. *6*, 20602.

Iatsenko, I., Boquete, J.P., and Lemaitre, B. (2018). Microbiota-derived lactate activates production of reactive oxygen species by the intestinal NADPH oxidase Nox and shortens Drosophila lifespan. Immunity *49*, 929–942.e5.

Ja, W.W., Carvalho, G.B., Mak, E.M., de la Rosa, N.N., Fang, A.Y., Liong, J.C., Brummel, T., and Benzer, S. (2007). Prandiology of Drosophila and the CAFE assay. Proc. Natl. Acad. Sci. U S A *104*, 8253–8256.

Ja, W.W., Carvalho, G.B., Zid, B.M., Mak, E.M., Brummel, T., and Benzer, S. (2009). Water- and nutrient-dependent effects of dietary restriction on Drosophila lifespan. Proc. Natl. Acad. Sci. U S A *106*, 18633–18637.

Kuo, C.F., Grainge, M.J., Zhang, W., and Doherty, M. (2015). Global epidemiology of gout: prevalence, incidence and risk factors. Nat. Rev. Rheumatol. *11*, 649–662.

Kuzuya, M., Ando, F., Iguchi, A., and Shimokata, H. (2002). Effect of aging on serum uric acid levels: longitudinal changes in a large Japanese population group. J. Gerontol. A Biol. Sci. Med. Sci. *57*, M660–M664.

Lang, S., Hilsabeck, T.A., Wilson, K.A., Sharma, A., Bose, N., Brackman, D.J., Beck, J.N., Chen, L., Watson, M.A., Killilea, D.W., et al. (2019). A conserved role of the insulin-like signaling pathway in diet-dependent uric acidpathologies in Drosophila melanogaster. PLoS Genet. *15*, e1008318.

Lee, K.-A., Kim, S.-H., Kim, E.-K., Ha, E.-M., You, H., Kim, B., Kim, M.-J., Kwon, Y., Ryu, J.-H., and Lee, W.-J. (2013). Bacterial-derived uracil as a modulator of mucosal immunity and gut-microbe homeostasis in Drosophila. Cell *153*, 797–811.

Li, M., Yang, D., Mei, L., Yuan, L., Xie, A., and Yuan, J. (2014). Screening and characterization of purine nucleoside degrading lactic acid bacteria isolated from Chinese sauerkraut and evaluation of the serum uric acid lowering effect in hyperuricemic rats. PLoS One *9*, e105577.

Lyngdoh, T., Marques-Vidal, P., Paccaud, F., Preisig, M., Waeber, G., Bochud, M., and Vollenweider, P. (2011). Elevated serum uric acid is associated with high circulating inflammatory cytokines in the population-based colaus study. PLoS One *6*, e19901.

Ma, Z., Wang, H., Cai, Y., Wang, H., Niu, K., Wu, X., Ma, H., Yang, Y., Tong, W., Liu, F., et al. (2018). Epigenetic drift of H3K27me3 in aging links glycolysis to healthy longevity in Drosophila. Elife *7*, e35368.

Meisinger, C., Koenig, W., Baumert, J., and Döring, A. (2008). Uric acid levels are associated with all-cause and cardiovascular disease mortality independent of systemic inflammation in men from the general population the MONICA ORA cohort study. Arterioscler. Thromb. Vasc. Biol. *28*, 1186–1192.

Miguel-Aliaga, I., Jasper, H., and Lemaitre, B. (2018). Anatomy and physiology of the digestive tract of drosophila melanogaster. Genetics *210*, 357–396.

Myllymäki, H., Valanne, S., and Rämet, M. (2014). The Drosophila Imd signaling pathway. J. Immunol. *192*, 3455–3462.

Obata, F., Fons, C.O., and Gould, A.P. (2018). Early-life exposure to low-dose oxidants can increase longevity via microbiome remodelling in Drosophila. Nat. Commun. *9*, 975.

Pan, L., Han, P., Ma, S., Peng, R., Wang, C., Kong, W., Cong, L., Fu, J., Zhang, Z., Yu, H., et al. (2019). Abnormal metabolism of gut microbiota reveals the possible molecular mechanism of nephropathy induced by hyperuricemia. Acta Pharm. Sin. B *10*, 249–261.

Shell, B.C., Schmitt, R.E., Lee, K.M., Johnson, J.C., Chung, B.Y., Pletcher, S.D., and Grotewiel, M. (2018). Measurement of solid food intake in Drosophila via consumption-excretion of a dye tracer. Sci. Rep. *8*, 11536.

Suez, J., and Elinav, E. (2017). The path towards microbiome-based metabolite treatment. Nat. Microbiol. *2*, 17075.

Tang, Z.-Z., Chen, G., Hong, Q., Huang, S., Smith, H.M., Shah, R.D., Scholz, M., and Ferguson, J.F. (2019). Multi-omic analysis of the microbiome and metabolome in healthy subjects reveals microbiome-dependent relationships between diet and metabolites. Front. Genet. *10*, 454.

van Dam, E., van Leeuwen, L.A.G., dos Santos, E., James, J., Best, L., Lennicke, C., Vincent, A.J., Marinos, G., Foley, A., Buricova, M., et al. (2020). Sugar-induced obesity and insulin resistance are uncoupled from shortened survival in Drosophila. Cell Metab. *31*, 710–725.e7.

Visconti, A., Le Roy, C.I., Rosa, F., Rossi, N., Martin, T.C., Mohney, R.P., Li, W., de Rinaldis, E., Bell, J.T., Venter, J.C., et al. (2019). Interplay between the human gut microbiome and host metabolism. Nat. Commun. *10*, 4505.

Wan, Y., Wang, F., Yuan, J., Li, J., Jiang, D., Zhang, J., Li, H., Wang, R., Tang, J., Huang, T., et al. (2019). Effects of dietary fat on gut microbiota and faecal metabolites, and their relationship with cardiometabolic risk factors: a 6-month randomised controlled-feeding trial. Gut *68*, 1417–1429.

Xi, Y., Yan, J., Li, M., Ying, S., and Shi, Z. (2019). Gut microbiota dysbiosis increases the risk of visceral gout in goslings through translocation of gut-derived lipopolysaccharide. Poult. Sci. *98*, 5361–5373.

Zheng, W., Rus, F., Hernandez, A., Kang, P., Goldman, W., Silverman, N., and Tatar, M. (2018). Dehydration triggers ecdysone-mediated recognition-protein priming and elevated anti-bacterial immune responses in Drosophila Malpighian tubule renal cells. BMC Biol. *16*, 60.

iScience, Volume *23*

Supplemental Information

Gut Bacterial Species Distinctively Impact Host Purine Metabolites during Aging in *Drosophila*

Toshitaka Yamauchi, Ayano Oi, Hina Kosakamoto, Yoriko Akuzawa-Tokita, Takumi Murakami, Hiroshi Mori, Masayuki Miura, and Fumiaki Obata

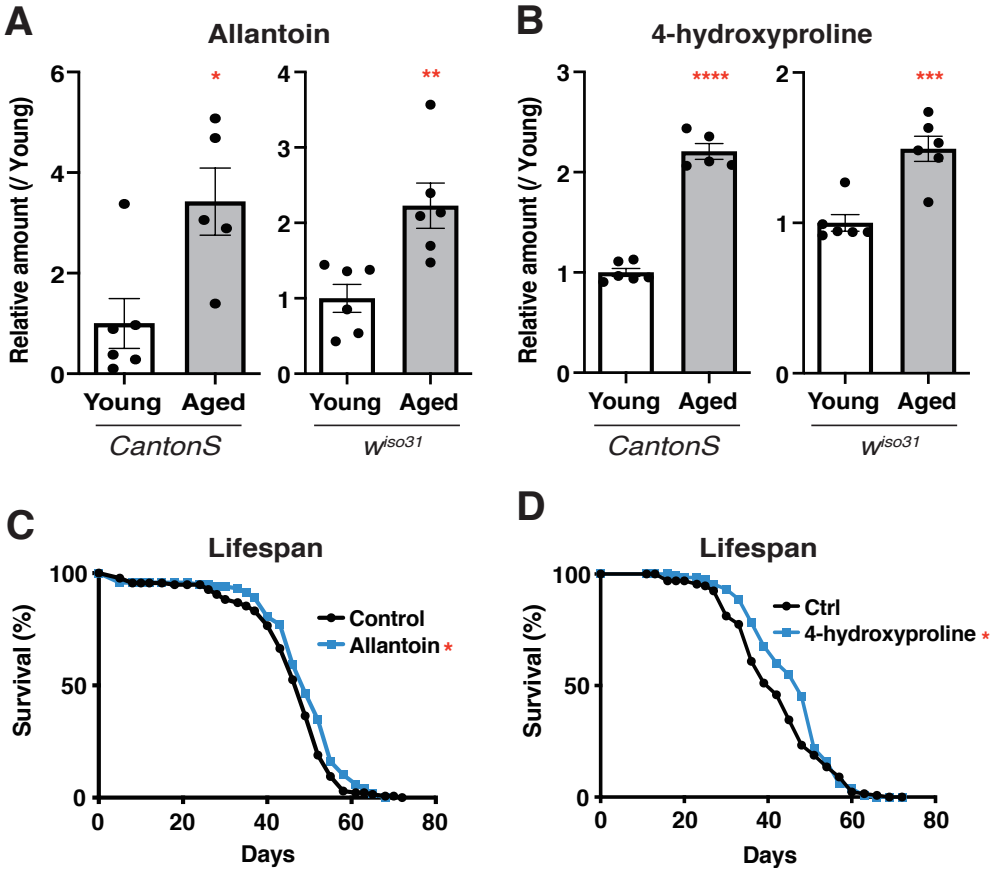

Figure S1. Allantoin and 4-hydroxyproline are robustly increased during aging, but they do not shorten lifespan. Related to Figure 1.

(A, B) Relative amount of allantoin or 4-hydroxyproline in whole body of aged (6-week-old) male flies (*CantonS, w^{iso31}*) compared to young (2-week-old) flies. n = 5–6. (C, D) Lifespan of w^{Dah} male flies fed with allantoin (1 mM) or 4-hydroxyproline (100 μg/mL). Concentration was determined based on the level of each metabolite in aged flies. n = 137 (Control), n = 118 (Allantoin) for (C). n = 133 (Control and 4-hydroxyproline) for (D). Log-rank test, $p < 0.05$. Data are represented as mean and SEM. Statistics, two-tailed Student's *t*-test. *, $p < 0.05$. **, $p < 0.01$. ***, $p < 0.001$. ****, $p < 0.0001$.

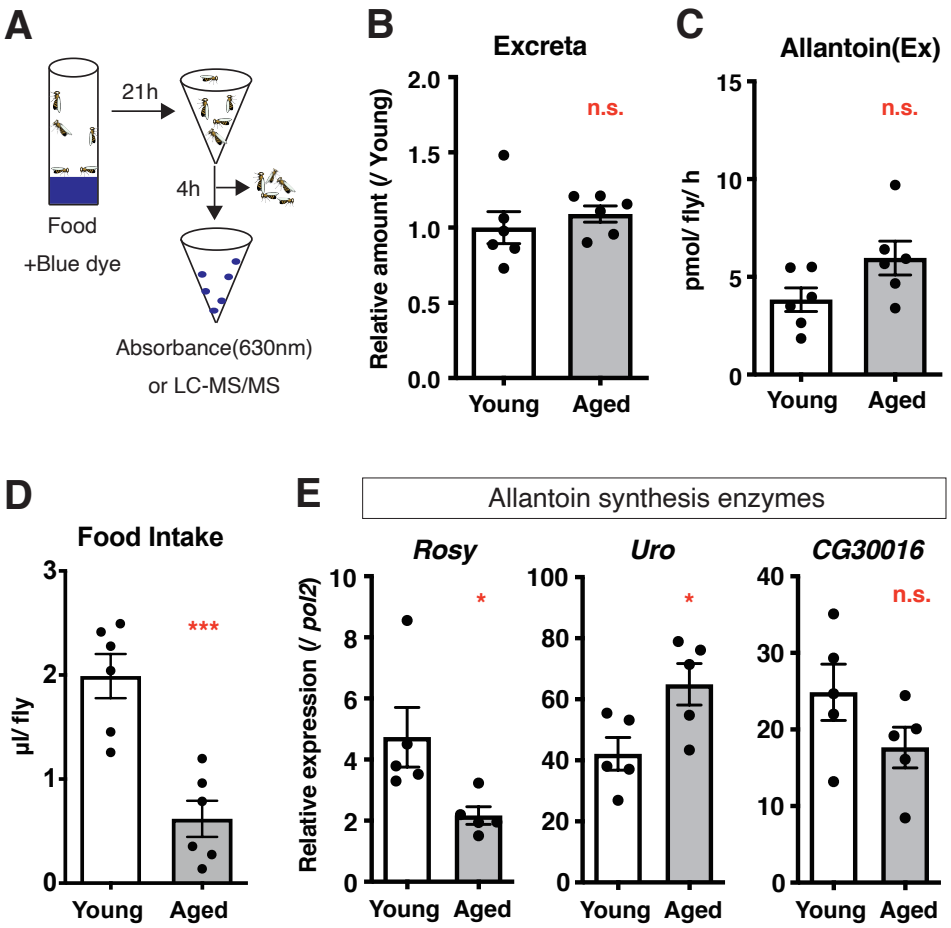

Figure S2. Quantification of excretion, food intake, and gene expression of enzymes for allantoin synthesis during aging. Related to Figure 2.

(A) Experimental scheme of excretion assay. (B) Amount of total excreta in aged (7-week-old) w^{Dah} male flies. Relative to young (1-week-old) w^{Dah} male flies. n = 6. (C) Quantification of allantoin by LC-MS/MS in excreta from young or aged w^{Dah} male flies. n = 6. (D) Quantification of food intake by the capillary feeder assay in young (2-week-old) and aged (5-week-old) w^{Dah} male flies. n = 6. (E) Quantitative RT-PCR of *Rosy, Urate oxidase* (*Uro*) *and CG30016* in the Malpighian tubules of young (1-week-old) or aged (7-week-old) w^{Dah} male flies. n = 5. Data are represented as mean and SEM. Statistics, two-tailed Student's *t*-test. *, $p < 0.05$. ***, $p < 0.001$.

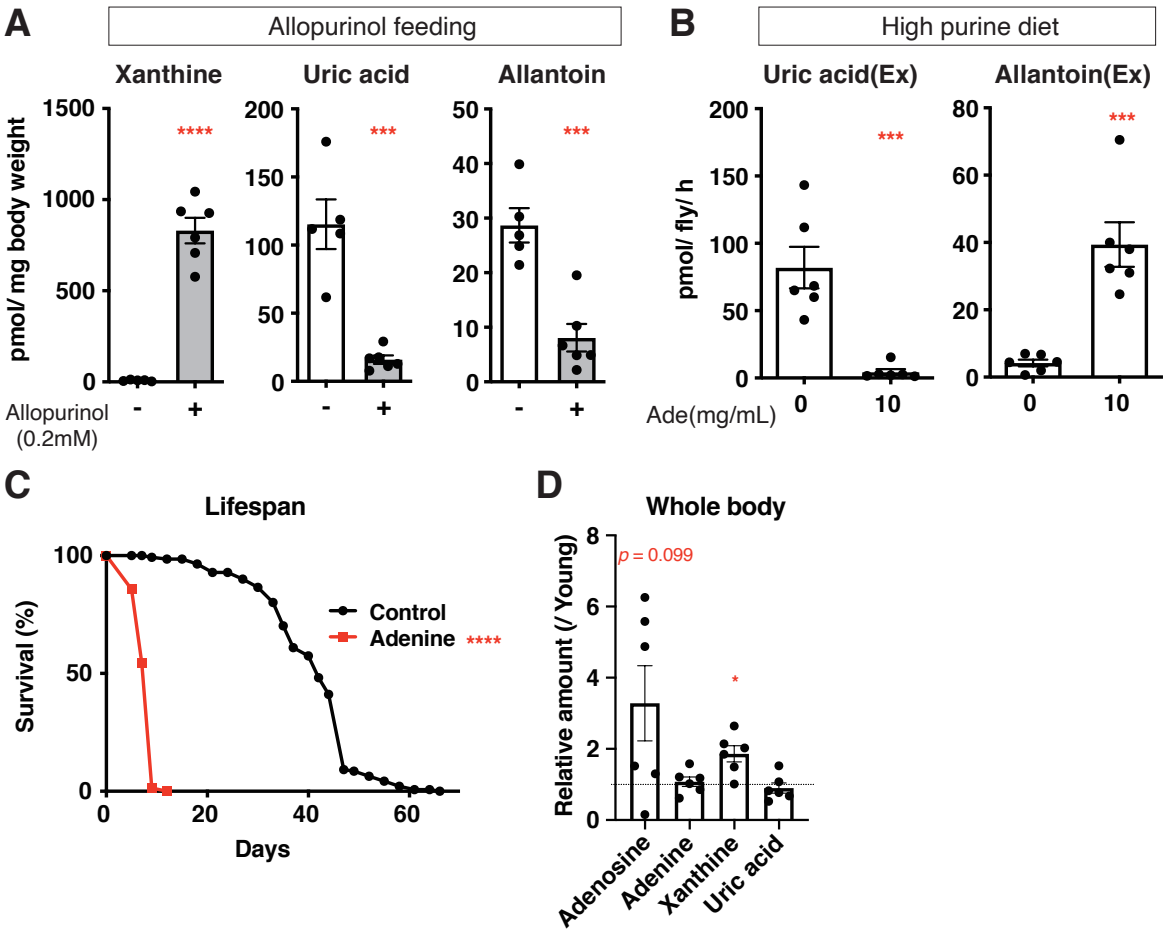

Figure S3. The amount of purine metabolites upon allopurinol, high-purine diet, or during aging. Related to Figure 2.

(A) Quantification of xanthine, uric acid and allantoin in whole body of young (1-week-old) w^{Dah} male flies fed with allopurinol (0.2 mM) for three days. n = 5–6. (B) Quantification of uric acid and allantoin by LC-MS/MS in excreta from young (2-week-old) w^{Dah} male flies fed with high-purine diet (Adenine, 10 mg/mL). n = 6. (C) Lifespan of w^{Dah} male flies fed with high-purine diet (Adenine, 10 mg/mL). n = 135 (Control), n = 147 (Adenine). Log-rank test, $p < 0.0001$. (D) Relative amount of adenosine, adenine, xanthine or uric acid by LC-MS/MS in whole body of aged (5-week-old) w^{Dah} male flies. Relative to young (1-week-old) flies. n = 6. Data are represented as mean and SEM. Statistics, two-tailed Student's *t*-test. *, $p < 0.05$. ***, $p < 0.001$. ****, $p < 0.0001$.

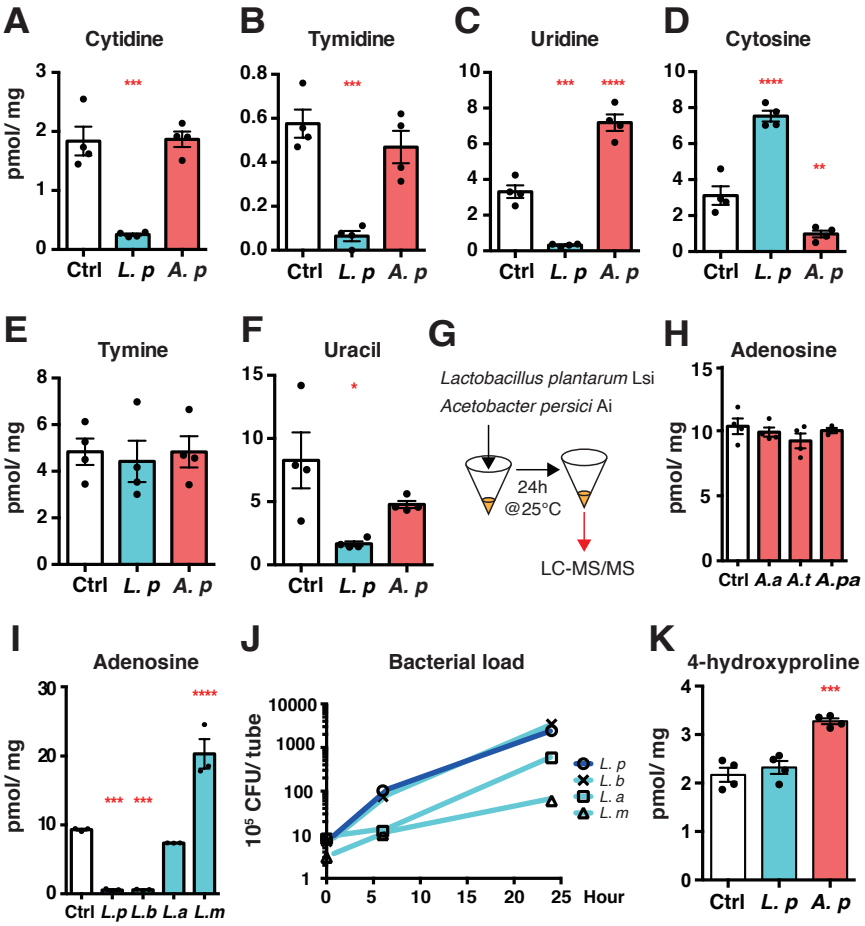

Figure S4. Bacteria modulate composition of fly diet in a species-specific manner. Related to Figure 4.

(A–F) Quantification of cytidine, tymidine, uridine, cytosine, tymine, and uracil by LC-MS/MS in fly diet conditioned with isolated bacteria strains. *L. p*, *L. plantarum* Lsi. *A. p*, *A. persici* Ai. Ctrl, control medium. n = 4. (G) Experimental scheme of bacterial conditioning assay in a 1.5 mL tube. (H, I) Quantification of adenosine by LC-MS/MS in fly diet conditioned with bacterial species. n = 4 for (H). *A.a*, *A. aceti* (NBRC 14818). *A.t*, *A. tropicalis* (NBRC 16470). *A.pa*, *A. pasteurianus* (NBRC 106471). n = 3 for (I). *L.p*, *L. plantarum* Lsi. *L.b*, *L. brevis* (NBRC 3345). *L.a*, *L. acidophilus* (NBRC 13951). *L.m*, *L. murinus* (NBRC 14221). (J) Colony forming unit (CFU) of four bacterial species (*L.p*, *L.b*, *L.a*, *L.m*) in fly diet. (K) Quantification of 4-hydroxyproline by LC-MS/MS in fly diet conditioned with isolated strains. n = 4. Data are represented as mean and SEM. Statistics, One-way ANOVA with Dunnett's multiple comparison test. *, $p < 0.05$, **, $p < 0.01$, ***, $p < 0.001$. ****, $p < 0.001$.

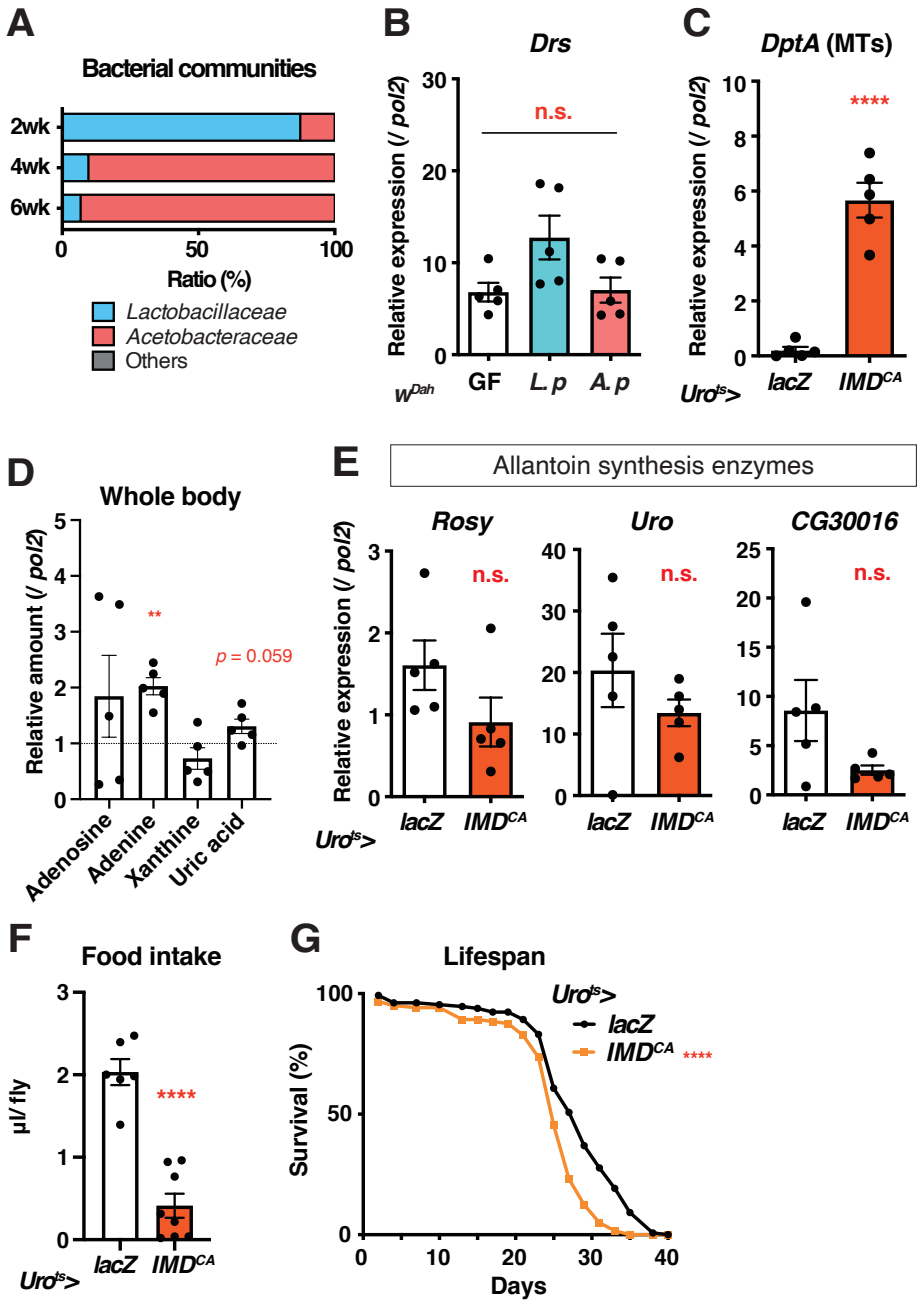

Figure S5. IMD activation, lifespan, and purine metabolism in the Malpighian tubules. Related to Figure 5 and 6.

(A) 16S rRNA amplicon sequencing analysis of gut microbiome in w^{iso31} flies. (B) Quantitative RT-PCR analysis of *Drosomycin* (*Drs*) in whole body of w^{Dah} young male flies mono-associated with the bacterial strains. *L. p*, *L. plantarum* Lsi. *A. p*, *A. persici* Ai. GF, Germ-free. n = 5. (C) Quantitative RT-PCR analysis of *Diptericin A* (*DptA*) of young male flies with ctrl (*lacZ*) or constitutive active form of IMD (IMD^{CA}) in the Malpighian tubules. n

= 5. (D) Relative amount of adenosine, adenine, xanthine or uric acid by LC-MS/MS in whole body of young (2-week-old) male flies fed with antibiotics. Either *lacZ* or IMD^{CA} was overexpressed in the Malpighian tubules. Relative to *lacZ* flies. $n = 5$. (E) Quantitative RT-PCR analysis of *Rosy, Urate oxidase* (*Uro*) *and CG30016* in the Malpighian tubules of young (2-week-old) male flies. Either *lacZ* or IMD^{CA} was overexpressed in the Malpighian tubules. $n = 5$. (F) Quantification of food intake by the capillary feeder assay in male flies. Either *lacZ* or IMD^{CA} was overexpressed in the Malpighian tubules. n = 6 (*lacZ*), n = 8 (IMD^{CA}). (G) Lifespan of male flies with overexpressing *lacZ* or IMD^{CA} in the Malpighian tubules. n = 130 (*lacZ*), n = 121 (IMD^{CA}). Log-rank test, $p < 0.0001$. Data are represented as mean and SEM. Statistics, One-way ANOVA with Dunnett's multiple comparison test (B) or two-tailed Student's *t*-test (C–F). ****, $p < 0.0001$.

Transparent Methods:

Fly husbandry and stock

Flies were reared on a standard diet containing 4 % cornmeal, 6 % baker's yeast (Saf Yeast), 6 % glucose (Wako, 042-31177), and 0.8 % agar (Kishida chemical, 260-01705) with 0.3 % propionic acid (Tokyo Chemical Industry, P0500) and 0.05 % nipagin (Wako, 132-02635). Flies were reared under 25 °C, 65 % humidity with 12 h/12 h light/dark cycles. The wild-type strains w^{Dah}, *Canton S* and w^{iso31} were used in the previous study (Obata et al., 2018). The fly lines were: *Da-GeneSwitch* (Dr. Veronique Monnier), *UAS-lacZ* (Dr. Goodman C), *UAS-IMD*^{CA} (Petkau et al., 2017), *NP1-Gal4, tub-Gal80*^{ts} (Jiang et al., 2009), *Uro-Gal4; tub-Gal80*^{ts} (Terhzaz et al., 2010), *Lpp-Gal4, tub-Gal80*^{ts}*/ TM6B* (Brankatschk and Eaton, 2010), *UAS-relish*-RNAi (BDSC: 33661), *UAS-Dredd*-RNAi (BDSC: 34070). *Da-GeneSwitch*, *UAS-lacZ* and *UAS-IMD*^{CA} are backcrossed with w^{iso31}. Adult flies eclosed within two days were collected and maintained for additional two days for maturation on standard diet. Then male flies were sorted with a density of 15 flies/ vial and flipped to fresh vials every three days. For lifespan analysis, the number of dead flies was counted every three days when flies were flipped to fresh vials.

Adult-specific genetic experiments were performed using *tub-Gal80*^{ts}. Flies were kept at 18 °C from embryo to adult flies and then shifted to 29 °C for six days or ten days. For GeneSwitch, RU486 (Wako, 84371-65-3) dissolved in ethanol (Wako, 052-00467) or the same amount of ethanol was added to standard diet to a final concentration of 200 μM, and flies were fed with the diet for six days.

Bacterial culture and strains

Isolated bacterial strains pre-cultured with MRS broth (Wako, 521-03485) for over night were cultured with the MRS broth for four to eight hours. Started OD_{600} was 0.01–0.1. Bacterial strains were: *L. plantarum* Lsi (Kosakamoto et al., 2020), *A. persici* Ai (Kosakamoto et al., 2020), *L. brevis* (NBRC3345), *L. acidophilus* (NBRC13951), *L. murinus* (NBRC14221), *A. aceti* (NBRC14818), *A. tropicalis* (NBRC16470), *A. pasteurianus* (NBRC106471). As for colony forming unit (CFU) count, obtained samples were scattered on MRS plate (OXOID, CM0361) and incubated at 30 °C for two days.

Dietary manipulations

High-purine diet was prepared by adding adenine hemisulfate (Sigma, A9126) to standard diet to a final concentration of two or ten mg/mL. For high-yeast feeding, male flies were fed with diet containing various concentrations of yeast extract (BD, 212750) in addition to 6 % glucose (Wako, 049-31165), 1 % agar, 0.3 % propionic acid, and 0.05 % nipagin for three days. For high-sugar feeding, male flies were fed with diet containing various concentrations of sucrose (Wako, 196-00015) in addition to 4 % yeast extract (BD, 212750), 1 % agar, 0.3 % propionic acid, and 0.05 % nipagin for three days. For allopurinol administration, male flies were fed with standard diet containing 0.2 mM allopurinol (Abcam, ab142565) for three days.

Bacterial manipulations

Antibiotics (200 μg/mL rifampicin, 50 μg/mL tetracycline, 500 μg/mL ampicillin) and 0.12 % nipagin were added to standard diet to remove all bacteria. To remove *Acetobacteraceae*, larvae were fed with 2.5 mM paraquat (1,1'-Dimethyl-4,4'-bipyridinium Dichloride, Tokyo Chemical Industry, D3685), and adult flies were collected in standard diet.

Germ-free flies were established by the bleach-based method. Embryos collected within four hours after egg laying were kept at 18 °C for overnight. The following day, larvae were carefully removed from collected embryos. Embryos were sterilized by 70 % ethanol three times and 3 % solution of sodium hypochlorites for five minutes. Embryos were then washed by sterilized water thoroughly. Embryos were transferred to vials containing antibiotics-supplemented diet (Ampicillin 50 μg/mL, Kanamycin 50 μg/mL, Tetracyclin 10 μg/mL, Erythromycin 10 μg/mL) for germ-free flies or vials containing UV-sterilized diet for mono-association of flies. For mono-association, 40 μL of bacterial culture (*L. plantarum* Lsi OD_{600} = 0.2, *A. persici* Ai OD_{600} = 0.02) was added directly on embryos. Gnotobiotic conditions of flies were constantly confirmed by plating on MRS agar.

Bacterial conditioning assay

For preparing bacterial-conditioned diet, *L. plantarum* or *A. persici*, 100 μL of cultured bacteria (OD_{600} = 0.2) was added on top of the standard diet (3 mL in fly vial) and incubated at 25 °C with 65 % humidity. Twenty-four hours later, the upper half of the conditioned diet

(30–50 mg) was collected and the composition was analysed by LC-MS/MS. For feeding flies with the bacterial-conditioned diet, 100 µL of the antibiotics-cocktail (10 mg/mL rifampicin, 2.5 mg/mL tetracycline and 25 mg/mL ampicillin) dissolved in 0.1N HCl was added to the bacterial-conditioned diet to inhibit/kill the proliferation of bacteria. We fed the flies with this diet for three days. For bacterial conditioning in a 1.5 mL tube, 2 µL of cultured bacteria (OD_{600} = 0.2) were added to the 30–50 mg of standard diet in a 1.5 mL tube. After 24 hours with 25 °C, 65 % humidity, the diet in the tube was analysed by LC-MS/MS or subjected to CFU count.

Quantitative RT-PCR analysis of immune activation or enzymes for purine metabolism

Total RNA was purified from four male flies or five to eight male Malpighian tubules using ReliaPrep RNA Tissue Miniprep kit (Promega, z6112). cDNA was prepared from 100–400 ng of the total RNA by the Takara PrimeScript RT Reagent Kit with gDNA Eraser (Takara bio, RR047). Quantitative PCR was performed using TB Green™ Premix Ex Taq™ (Tli RNaseH Plus, Takara bio, RR820W) and a Quantstudio 6 Flex Real Time PCR system (ThermoFisher) using *RNA pol2* as an internal control. Primer sequences were:

RNA pol2 forward, CCTTCAGGAGTACGGCTATCATCT.

RNA pol2 reverse, CCAGGAAGACCTGAGCATTAATCT.

Rosy forward, TGGTGACTTCCCACTGGAG.

Rosy reverse, GGTTCGGGTATTTCAAGCAG.

Uro forward, GCGATGTGGTTATAAGGAGAACA.

Uro reverse, TCTTCAGCACCCGGAGAC.

CG30016 forward, GATGCACGAAAGTTTTCTACCC.

CG30016 reverse, GGGATCTCCATTCCTGAATCT.

DptA forward, CGTCGCCTTACTTTGCTGC.

DptA reverse, CCCTGAAGATTGAGTGGGTACTG.

16S rRNA gene amplicon sequencing analysis

Flies were rinsed in 3 % bleach, 70 % ethanol and then washed extensively with PBS before dissection. Dissected guts (four guts per sample) were collected in PBS on ice, then

transferred to 270 μL lysis buffer (20 mM Tris pH8.0, 2 mM EDTA and 1% Triton X-100) with 20 mg/mL lysozyme from chicken egg (Sigma, L4919) and homogenized. Homogenized samples were stored at -80 °C. Frozen gut samples were thawed at 37 °C for 45 min in a 1.5 mL microcentrifuge tube, transferred to a 2 mL tube containing 0.1 mm glass beads (Scientific Industries, SI-BG01) and then incubated using a Mini-Beadbeater-24 (Biospec Products, 112011EUR) at 2,500 rpm for 20 s. After 15 min incubation at 37 °C, 30 μL of proteinase K and 200 μL Buffer TL (Qiagen) were added to each sample, followed by incubation at 56 °C for 15 min. Genomic DNA was purified by QIAamp DNA Micro kit (Qiagen, 56304), and V3–V4 variable region of 16S rRNA genes were amplified using 341f/806r primer set. PCR amplicons were purified using a QIAquick PCR Purification kit (Qiagen, 28104) and sent to Fasmac for Illumina MiSeq sequencing and analysis. The data were deposited to DDBJ (accession number, DRA 010501).

Genome analysis of *Lactobacilli*

Protein-coding sequences (CDSs) within the genomes of four *Lactobacillus* species were predicted and annotated by using DFAST pipeline with the Prodigal option (Hyatt et al., 2010; Tanizawa et al., 2018). In addition to the DFAST annotation, KEGG orthology identifiers were assigned to the CDSs by conducting BLASTP search against KEGG protein database (Kanehisa et al., 2014) with the following criteria: sequence identity ≥ 40 %, e-value < 1e-5, bit score ≥ 70, and aligned region covering 40 % and more of both query and subject sequences. Deduced CDSs among the four species were then clustered into homologous gene groups by using OrthoFinder v2.3.8 (Emms and Kelly, 2019).

Measurement of metabolites or diet composition

Liquid chromatography-tandem mass spectrometry (LC-MS/MS) was used to analyse fly metabolites and diet composition. Four or five whosle bodies of adult male flies or 30–50 mg of bacterial-conditioned diet were homogenized in 160 μL of 80 % methanol containing 10 μM of internal standards (methionine sulfone and 2-morpholinoethanesulfonic acid), then de-proteinised by 75 μL acetonitrile and 10 kDa column, followed by complete evaporation. The samples were resolubilised in water and injected to LC-MS/MS with PFPP column (Discovery HS F5 (2.1 mm x 150 mmL, 3 μm, Sigma-Aldrich) in the column oven at 40 °C. Gradient from solvent A (0.1 % formic acid, Water) to solvent B (0.1 % formic acid, acetonitrile) were

performed during 20 minutes of analysis. MRM methods for metabolite quantification were optimised using the software (Labsolutions, Shimazu). The data was normalized by methionine sulfone and wet weight of the sample. The Heat map and PLS-DA analyses were conducted by MetaboAnalyst 4.0 with the data after auto scaling (Chong et al., 2019).

Excretion assay

Flies were transferred onto standard diet containing 2 % blue dye (Brilliant blue FCF, Wako, 3844-45-9) at 25 °C, 65 % humidity for 21 hours. Five flies were then transferred to a 1.5 mL tube containing 20 μL of 1 % sucrose, 1 % agar and incubated for four hours. To collect excreta, 50 μL of water was added to the 1.5mL tube and dissolve by vortex, followed by measuring absorbance at 630 nm. To quantify metabolites by LC-MS/MS, excreta was collected by 300 μL of 80 % methanol containing 10 μM of internal standards (methionine sulfone and 2-morpholinoethanesulfonic acid). The samples were then subjected to the standard procedure for LC-MS/MS analysis as described above.

Purine or pyrimidine-depleted bacteria medium

We adapted a previously-reported chemically defined medium (Piper et al., 2017) for bacterial culture with following modifications. Cholesterol and agar were not included. To prevent precipitation, metal irons were reduced to one tenth of the original concentrations. For purine- or pyrimidine-depleted medium, inosine or uridine was depleted respectively. To assess the bacterial growth speed, bacteria precultured with purine/pyrimidine-depleted medium (OD_{600} = 0.02) were added in the corresponding medium and incubated at 30 °C for 21 hours.

Capillary feeder assay

Two glass capillaries containing 5 % yeast extract, 2 mg/mL red dye (Acid red 52, Wako, 3520-42-1), and n-Octyl acetate (1:100,000; TCI, 112-14-1) were inserted into the cap. Ten male flies were placed in each empty vial. The level of the food was marked, and the vials were laid in a container with wet towels to prevent water evaporation. The container was

incubated at 25 °C. After 24 hours, the amount of the food remained in the capillaries was recorded. The vial without flies was also included in the container to subtract evaporation.

Quantification and statistical analysis

Statistical analysis was performed using Graphpad Prism 8 except for survival curves where OASIS2 was used (Han et al., 2016). A two-tailed Student's *t*-test was used to test between two samples. One-way ANOVA with multiple comparison tests was used to compare among group. Statistical significance is; *, $p < 0.05$, **, $p < 0.01$, ***, $p < 0.001$, ****, $p < 0.0001$. Bar graphs were drawn as mean and SEM with all the data point shown by dots to allow readers to see the number of samples and each raw data.

Supplemental References:

Brankatschk, M., and Eaton, S. (2010). Lipoprotein particles cross the blood-brain barrier in Drosophila. J. Neurosci. *30*, 10441–10447.

Chong, J., Wishart, D.S., and Xia, J. (2019). Using MetaboAnalyst 4.0 for Comprehensive and Integrative Metabolomics Data Analysis. Curr. Protoc. Bioinforma. *68*, e86.

Emms, D.M., and Kelly, S. (2019). OrthoFinder: Phylogenetic orthology inference for comparative genomics. Genome Biol. *20*, 238.

Han, S.K., Lee, D., Lee, H., Kim, D., Son, H.G., Yang, J.S., Lee, S.J. V., and Kim, S. (2016). OASIS 2: Online application for survival analysis 2 with features for the analysis of maximal lifespan and healthspan in aging research. Oncotarget *7*, 56147.

Hyatt, D., Chen, G.L., LoCascio, P.F., Land, M.L., Larimer, F.W., and Hauser, L.J. (2010). Prodigal: Prokaryotic gene recognition and translation initiation site identification. BMC Bioinformatics *11*, 119.

Jiang, H., Patel, P.H., Kohlmaier, A., Grenley, M.O., McEwen, D.G., and Edgar, B.A. (2009). Cytokine/Jak/Stat Signaling Mediates Regeneration and Homeostasis in the Drosophila Midgut. Cell *137*, 1343–1355.

Kanehisa, M., Goto, S., Sato, Y., Kawashima, M., Furumichi, M., and Tanabe, M. (2014). Data, information, knowledge and principle: back to metabolism in KEGG. Nucleic Acids Res. *42*, D199–D205.

Kosakamoto, H., Yamauchi, T., Akuzawa-Tokita, Y., Nishimura, K., Soga, T., Murakami, T., Mori, H., Yamamoto, K., Miyazaki, R., Koto, A., et al. (2020). Local Necrotic Cells Trigger Systemic Immune Activation via Gut Microbiome Dysbiosis in Drosophila. Cell Rep. *32*, 107938.

Obata, F., Fons, C.O., and Gould, A.P. (2018). Early-life exposure to low-dose oxidants can increase longevity via microbiome remodelling in Drosophila. Nat. Commun. *9*, 975.

Petkau, K., Ferguson, M., Guntermann, S., and Foley, E. (2017). Constitutive Immune Activity Promotes Tumorigenesis in Drosophila Intestinal Progenitor Cells. Cell Rep. *20*, 1784–1793.

Piper, M.D.W., Soultoukis, G.A., Blanc, E., Mesaros, A., Herbert, S.L., Juricic, P., He, X., Atanassov, I., Salmonowicz, H., Yang, M., et al. (2017). Matching Dietary Amino Acid Balance to the In Silico-Translated Exome Optimizes Growth and Reproduction without Cost to Lifespan. Cell Metab. *25*, 610–621.

Tanizawa, Y., Fujisawa, T., and Nakamura, Y. (2018). DFAST: a flexible prokaryotic genome annotation pipeline for faster genome publication. Bioinformatics *34*, 1037–1039.

Terhzaz, S., Cabrero, P., Chintapalli, V.R., Davies, S.A., and Dow, J.A.T. (2010). Mislocalization of mitochondria and compromised renal function and oxidative stress resistance in Drosophila SesB mutants. Physiol. Genomics *41*, 33–41.